Supplement of Geosci. Model Dev., 15, 4783–4803, 2022
https://doi.org/10.5194/gmd-15-4783-2022-supplement

Geoscientific Model Development
Open Access
EGU

Supplement of

Using terrestrial laser scanning to constrain forest ecosystem structure and functions in the Ecosystem Demography model (ED2.2)

Félicien Meunier et al.

Correspondence to: Félicien Meunier (felicien.meunier@ugent.be)

Supplementary material

Supplementary section S1: list of references extracted from TRY used in this study

(Diaz et al. 2004; Cornelissen 1996; Kleyer et al. 2008; Cornelissen, Diez, and Hunt 1996; Ogaya and Peñuelas 2003; Reich, Oleksyn, and Wright 2009; Cornwell et al. 2008; Wright et al. 2004; Cornelissen et al. 2003; Burrascano et al. 2015; Wirth and Lichstein 2009; Maire et al. 2015; Paine et al. 2015; Liebergesell et al. 2016; Shipley 2002; Ordoñez et al. 2010; Scherer-Lorenzen et al. 2007; Falster et al. 2015; Niinemets 2001; Garnier et al. 2007; Giarrizzo et al. 2017; Coomes et al. 2008; Kattge et al. 2009; Atkin et al. 2015; Medlyn et al. 1999; Milla and Reich 2011)

Supplementary section S2: supplementary results

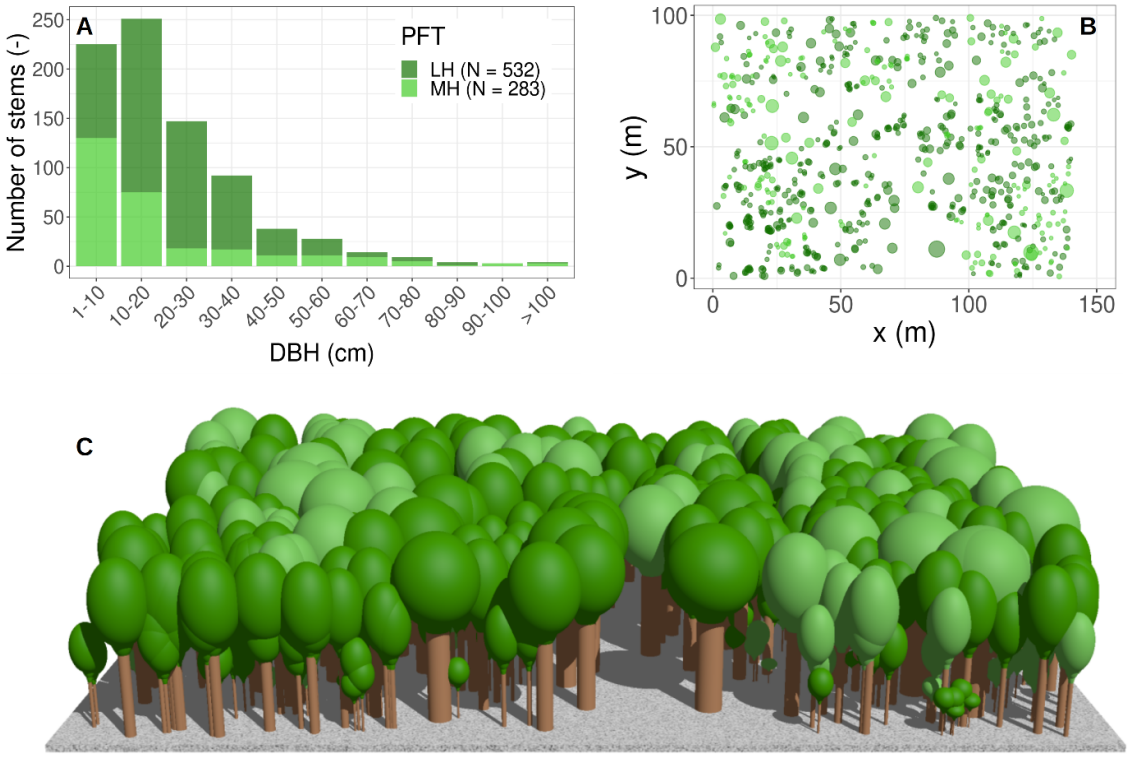

Figure S1: Initial conditions in terms of tree size distribution and PFT composition (A), horizontal position, basal area, and PFT composition (B), and a three-dimensional visualisation of the ecosystem PFT composition in ED2.2 (C). The PFT colour legend applies to all three panels.

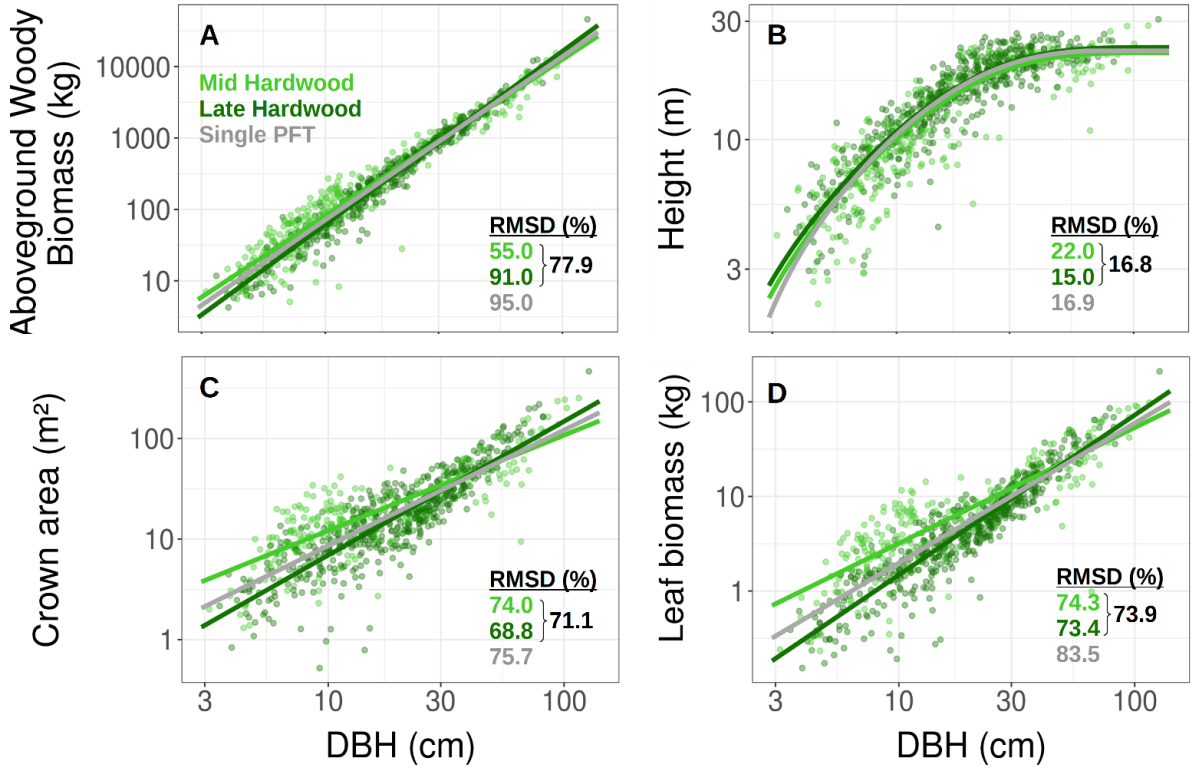

Figure S2: TLS-derived model allometries for the aboveground woody biomass (A), tree height (B), crown area (C), and leaf biomass (D) for either a single PFT (grey lines) or multiple PFTs (coloured lines). The data to which the TLS allometries were fitted (coloured points corresponding to the species-PFT classification of Table 1) were obtained using TLS. The root-mean-square deviation relative to the observed mean of each variable is also indicated for each model (grey: $N_{PFT} = 1$, black: $N_{PFT} = 2$) or PFT (shades of green). Coefficients used to plot the allometries can be found in Table 3.

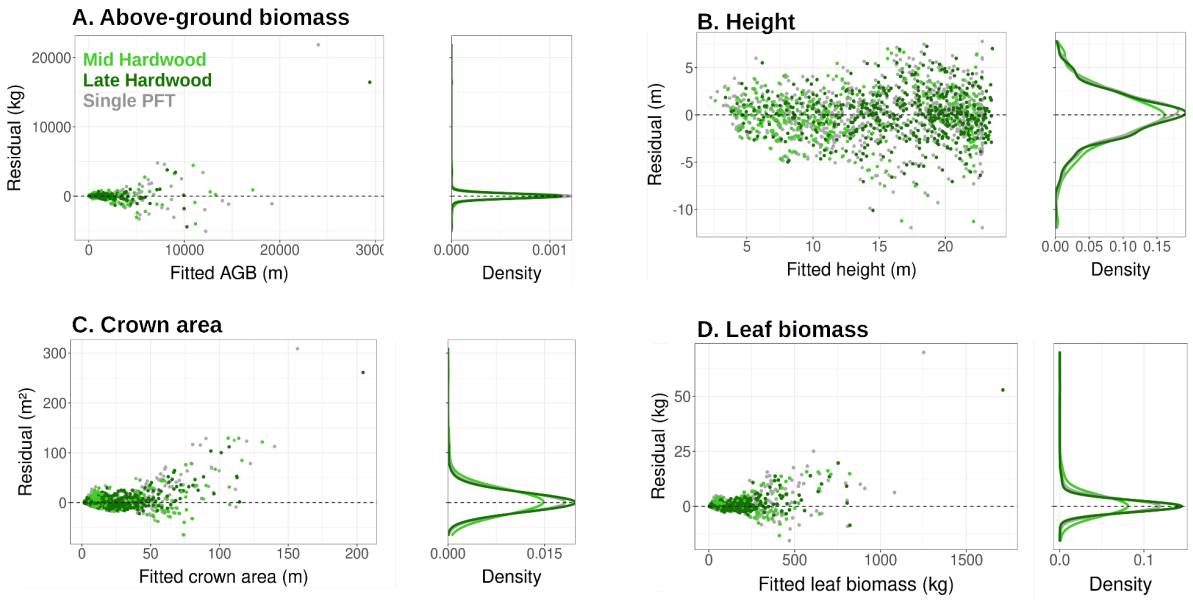

Figure S3: Residual plots of the woody biomass (A), tree height (B), crown area (C), and leaf biomass (D) allometric models using either a single PFT (grey dots and lines) or multiple PFTs (coloured dots and lines).

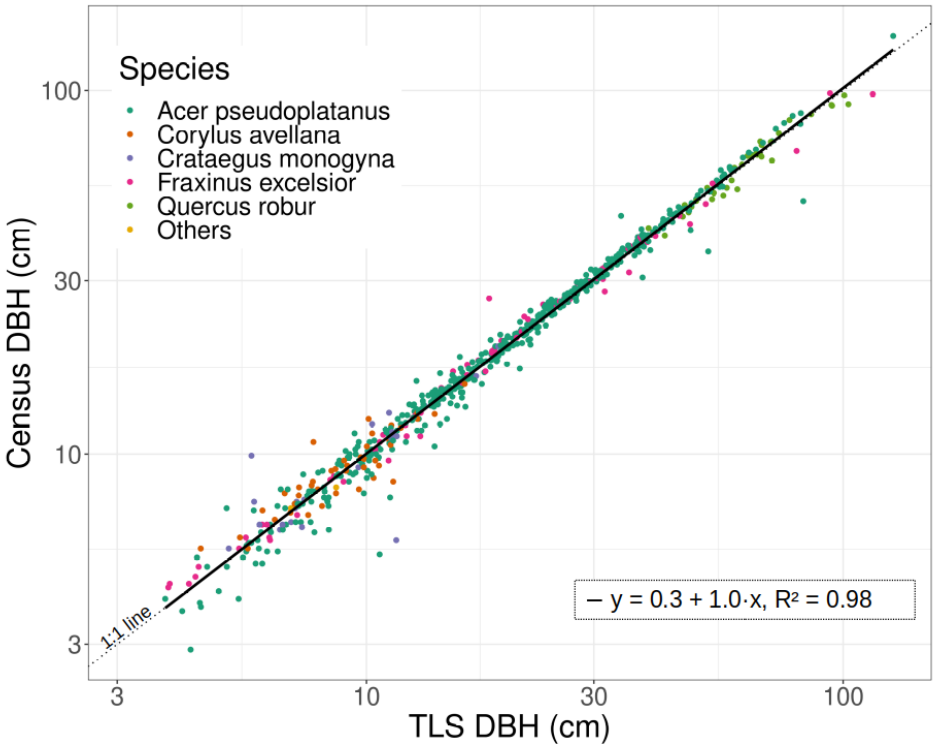

Figure S4: Comparison between field inventoried and TLS-derived DBH for all dominant tree species in the 1.4 ha plot in Wytham Woods (coloured dots).

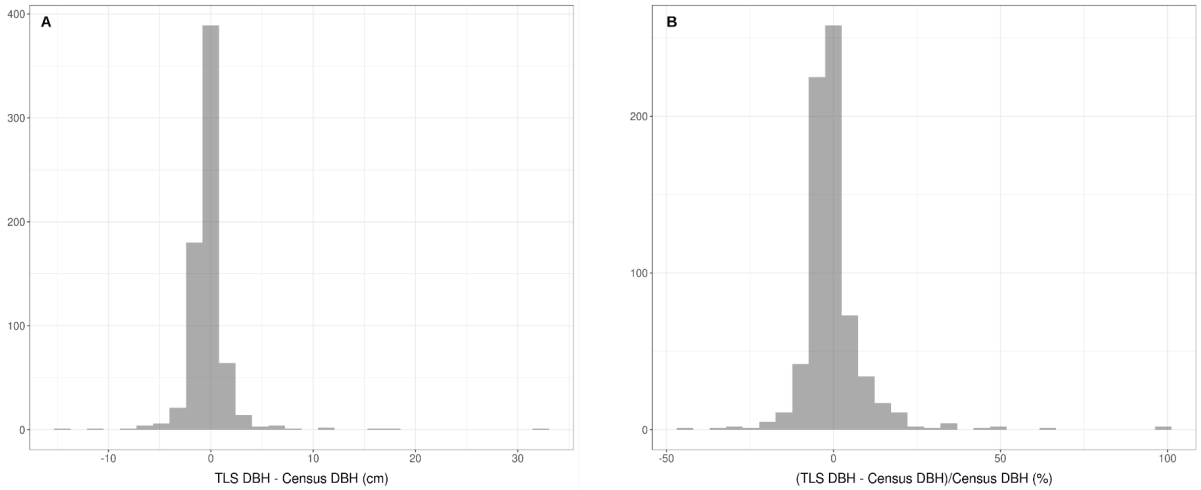

Figure S5: Distribution of the absolute (A) and relative (B) difference between TLS and field inventoried DBH for all trees in the 1.4 ha plot in Wytham Woods.

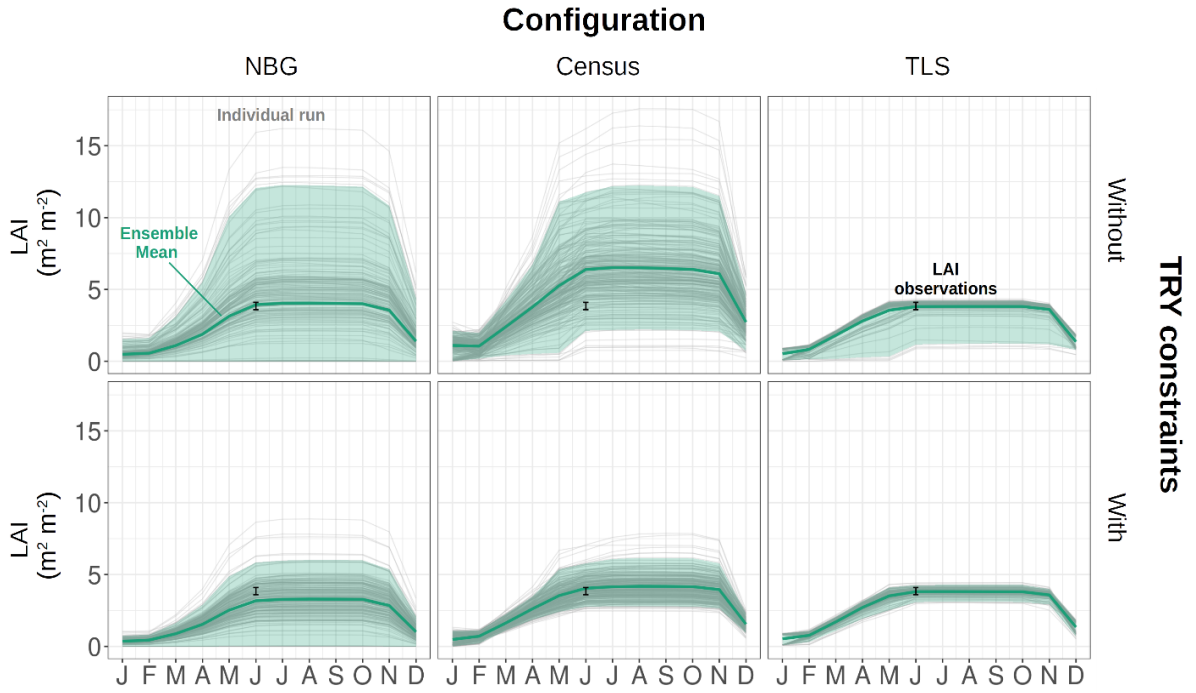

Figure S6: Seasonal cycle of the ecosystem LAI, as observed by independent observations (black range) or as simulated by ED2.2 for multiple model configurations (columns) and with or without TRY constraints on SLA and $V_{c,max}$ (rows). The green thick lines are the ensemble means while the shaded envelopes encompass 95% of the ensemble members. The individual ensemble members are also plotted as thin grey lines. The settings of the model configurations are detailed in Table 5.

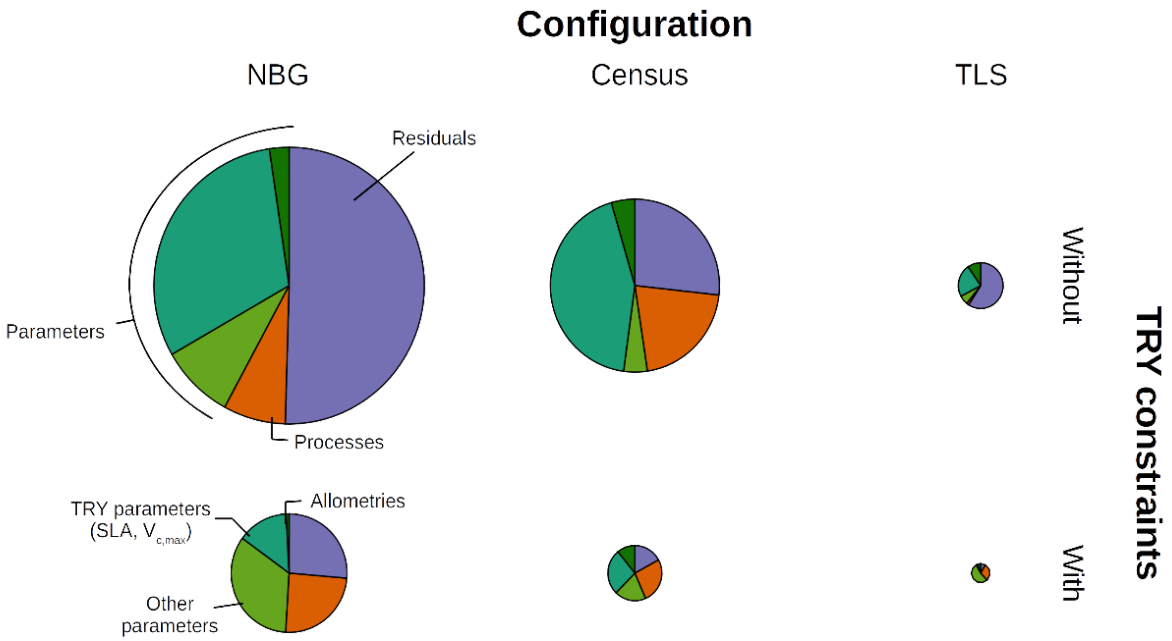

Figure S7: Decomposition of the simulated LAI variance into process (orange), parameter (green), and residual (mauve) uncertainty for multiple model configurations (columns) and with or without TRY constraints on SLA and $V_{c,max}$ (rows). The parameter uncertainty was further decomposed into the contribution of the allometric, TRY-constrainable (SLA and $V_{c,max}$), and other parameters (shades of green). The radii of the pie charts are proportional to the total variance of the ecosystem LAI in each configuration for the leaf-on season (May-October). The settings of the model configurations are detailed in Table 5.

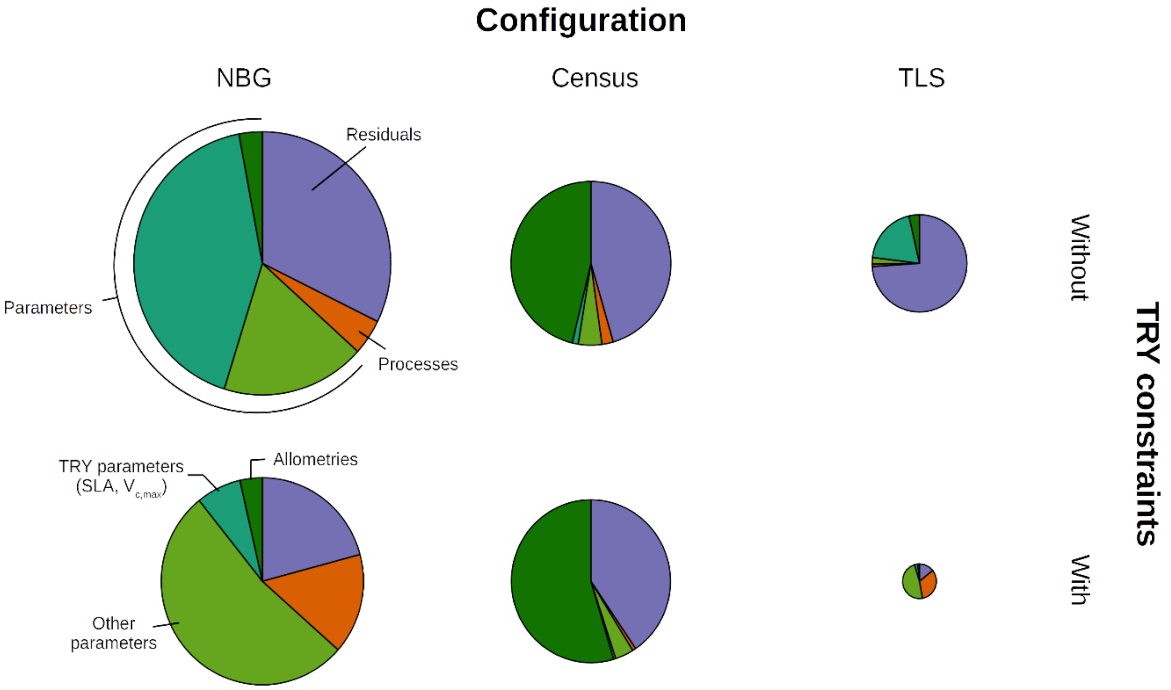

Figure S8: Decomposition of the simulated AGB variance into process (orange), parameter (green), and residual (mauve) uncertainty for multiple model configurations (columns) and with or without TRY constraints on SLA and $V_{c,max}$ (rows). The parameter uncertainty was further decomposed into the contributions of the allometric, TRY-constrainable (SLA and $V_{c,max}$), and other parameters (shades of green). The radii of the pie charts are proportional to the total variance of the final AGB in each configuration. The settings of the model configurations are detailed in Table 5.

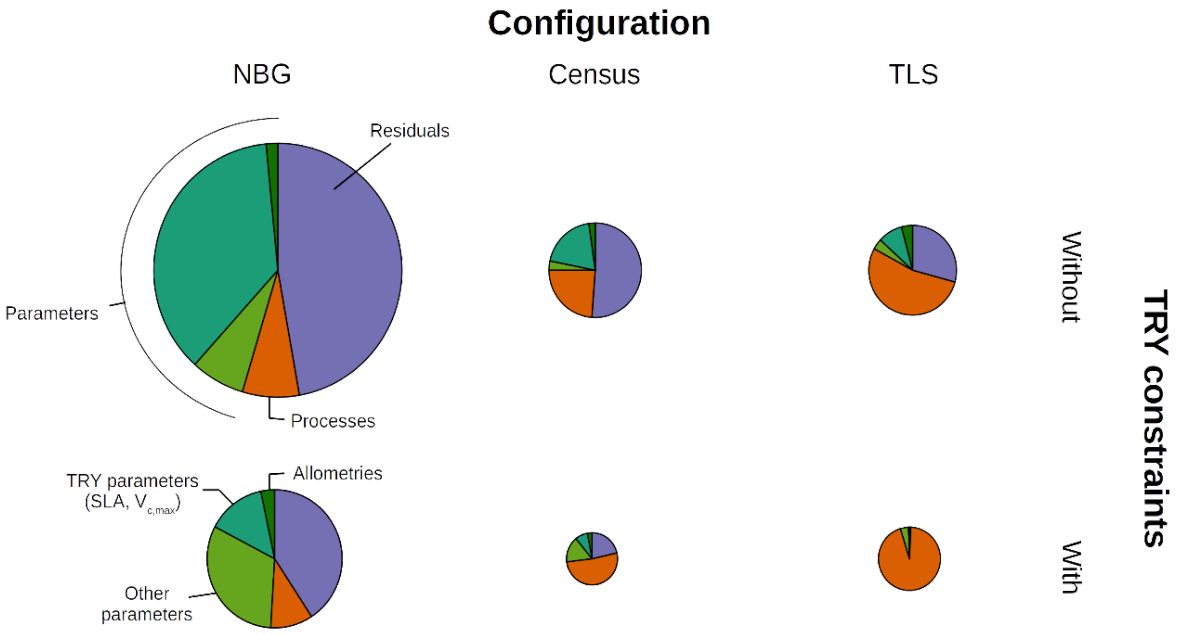

Figure S9: Decomposition of the simulated PAR variance into process (orange), parameter (green), and residual (mauve) uncertainty for multiple model configurations (columns) and with or without TRY constraints on SLA and $V_{c,max}$ (rows). The parameter uncertainty was further decomposed into the contributions of the allometric, TRY-constrainable (SLA and $V_{c,max}$), and other parameters (shades of green). The radii of the pie charts are proportional to the total variance of the PAR reaching the ground during the leaf-on season in each configuration. The settings of the model configurations are detailed in Table 5.